

# IDESplat: Iterative Depth Probability Estimation for Generalizable 3D Gaussian Splatting

Wei Long<sup>1</sup>, Haifeng Wu<sup>1</sup>, Shiyin Jiang<sup>1</sup>, Jinhua Zhang<sup>1</sup>, Xinchun Ji<sup>2</sup>, Shuhang Gu<sup>1\*</sup>

<sup>1</sup>University of Electronic Science and Technology of China

<sup>2</sup>Chinese Academy of Sciences

lwsch5940@163.com, shuhanggu@gmail.com

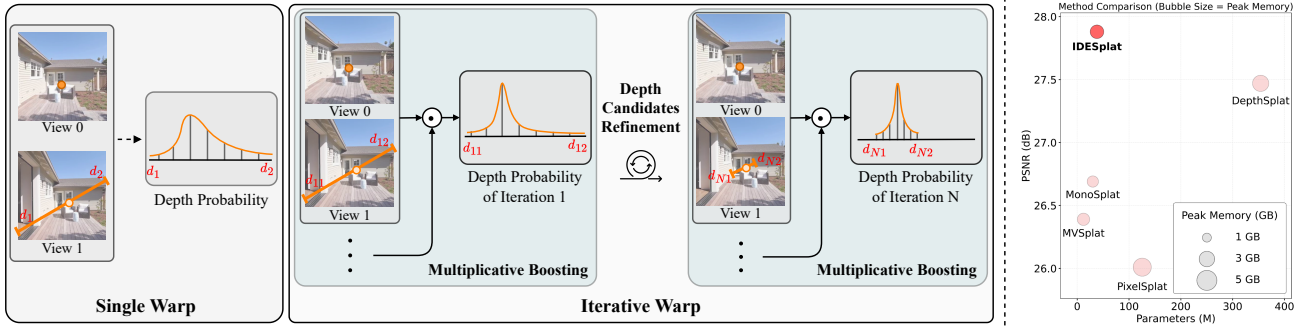


Figure 1. **Left:** Methods [5, 22, 46] that estimate depth probability via a single warp operation. **Middle:** Our IDESpLat can iteratively leverage multi-warp operations to boost the depth probability estimate and refine the depth candidates for accurate Gaussian mean predictions. **Right:** The experimental results of our IDESpLat compared with mainstream methods such as PixelSplat [2], MVSplat [5], MonoSplat [22], and DepthSplat [46]. The PSNR values are reported for the entire RE10K test set.

## Abstract

Generalizable 3D Gaussian Splatting aims to directly predict Gaussian parameters using a feed-forward network for scene reconstruction. Among these parameters, Gaussian means are particularly difficult to predict, so depth is usually estimated first and then unprojected to obtain the Gaussian sphere centers. Existing methods typically rely solely on a single warp to estimate depth probability, which hinders their ability to fully leverage cross-view geometric cues, resulting in unstable and coarse depth maps. To address this limitation, we propose **IDESplat**, which iteratively applies warp operations to boost depth probability estimation for accurate Gaussian mean prediction. First, to eliminate the inherent instability of a single warp, we introduce a *Depth Probability Boosting Unit (DPBU)* that integrates epipolar attention maps produced by cascading warp operations in a multiplicative manner. Next, we construct an iterative depth estimation process by stacking multiple DPBUs, progressively identifying potential depth candidates with high likelihood. As IDESpLat iteratively boosts depth probability estimates and updates the depth candidates, the depth map is gradually refined, resulting in accurate Gaussian means. We conduct experiments on *RealEstate10K*, *ACID* and *DL3DV*.

\*corresponding author

*IDESplat achieves outstanding reconstruction quality and state-of-the-art performance with real-time efficiency. On RE10K, it outperforms DepthSplat by 0.33 dB in PSNR, using only 10.7% of the parameters and 70% of the memory. Additionally, our IDESpLat improves PSNR by 2.95 dB over DepthSplat on the DTU dataset in cross-dataset experiments, demonstrating its strong generalization ability. The code is available at [here](#).*

## 1. Introduction

Single-scene 3D Gaussian Splatting (3DGS) benefits from a rasterization-friendly pipeline, making it well-suited for real-time scene reconstruction [17, 51], but it suffers from limited generalization capabilities. Generalizable 3DGS [2, 5, 21, 46, 53] addresses this shortcoming by using a feed-forward network to directly predict all Gaussian parameters, enabling it to handle unseen scenes. Among all the Gaussian sphere parameters, the Gaussian mean is crucial but difficult to predict directly due to the local support nature of Gaussian gradients [2], which significantly affects the optimization of the overall parameters. Existing methods [5, 22, 46, 52] commonly require first estimating the pixel-wise depth map and then unprojecting it to obtain the centers of the Gaussian spheres. This design reduces the difficulty of the network op-

timization process by decoupling the prediction of Gaussian mean parameters, while increasing the reliance on accurate depth estimation.

Efforts have been made to obtain accurate and refined depth estimation. Early methods [2, 34] directly use differentiable operations to predict the depth probability distribution from image features. Although these methods can predict the depth map for scene reconstruction in a generalizable way, their ability to exploit multi-view feature similarity is limited, which restricts their performance. Subsequent approaches [5, 21] introduce cost volumes that use warp operations to establish feature similarity across views, which provide valuable geometric cues for depth estimation and simplify the network learning process. However, these methods rely solely on a single warp to model feature similarity, which prevents them from fully exploiting the rich geometric information, leading to unstable and coarse depth maps. Therefore, how to incorporate multiple warps to gradually leverage rich cross-view geometric details, producing refined and reliable depth maps for accurate Gaussian mean prediction, remains a key challenge.

In this paper, we propose IDESplat, which iteratively performs warps to refine depth maps for accurate Gaussian means prediction. By integrating cascade warp results, we can progressively boost the feature similarity measure to identify high-likelihood surface points and suppress low-probability depth candidates. The iterative warp framework of our IDESplat is shown in Fig. 1. Firstly, to eliminate the instability of a single warp, we introduce a Depth Probability Boosting Unit (DPBU) to fuse multiple epipolar attention maps in a multiplicative manner for a reliable depth map. Next, we gradually update the depth search range while increasing the feature resolution, enabling warp and correlation calculations at a finer scale. Feature matching becomes easier and more precise as the depth search range is re-centered and image features are enhanced in this process. Finally, for other Gaussian parameters, we propose a Gaussian Focused Module that determines the most relevant Gaussian tokens to compute attention weights for feature interaction. The experimental results on RealEstate10K show that IDESplat outperforms DepthSplat by **0.33 dB** in PSNR with only **10.7%** of the parameters and **70%** of the memory. Moreover, IDESplat shows outstanding cross-dataset generalization, achieving 28.79 dB on ACID when transferred from RE10K, outperforming methods trained directly on ACID. It also improves PSNR by **2.95 dB** over DepthSplat on the DTU dataset in cross-dataset experiments. In summary, the main contributions of this paper are as follows:

- We propose IDESplat, a generalizable feedforward 3DGS model, which iteratively performs warps to progressively boost the feature similarity measure and refine depth maps for accurate Gaussian mean prediction.
- To eliminate the inherent instability of a single warp, we

introduce a Depth Probability Boosting Unit that multiplicatively integrates multiple epipolar attention maps for reliable and refined depth map estimation.

- We design a Gaussian Focused Module to identify the most relevant Gaussian tokens for computing attention scores and reweight enhanced features.
- Experiments on RealEstate10K ACID, and DL3DV show that our IDESplat significantly improves reconstruction quality and generalization capability while maintaining real-time inference efficiency.

## 2. Related Work

**Generalizable 3D Gaussian Splatting.** Single-scene 3D Gaussian Splatting methods [9, 10, 17, 28, 47] achieve more efficient rendering than neural fields and volume rendering methods [23, 26, 31, 40] due to their rasterization-friendly properties, but are still constrained by long optimization times and limited generalization capabilities. Generalizable 3D Gaussian Splatting methods [2, 22, 35, 46] address this issue through single-pass feed-forward prediction of all Gaussian parameters within a scene, enabling fast modeling of unseen scenes and view synthesis. Early studies [2, 34] used feed-forward neural networks to directly predict Gaussian parameters from image features, enabling generalizable scene reconstruction. Since the introduction of cost volume computation to generalizable 3DGS, many studies [5, 21] have focused on extracting geometric cues from cross-view images to enhance depth estimation accuracy, thereby simplifying the optimization of Gaussian parameters. Subsequently, recognizing the importance of accurate depth estimation, some methods [22, 46] have incorporated pre-trained monocular depth models, leading to significant performance improvements. However, Existing methods rely on a single warp for depth estimation, limiting their ability to exploit cross-view feature cues. In contrast, our IDESplat integrates feature similarity from cascaded warps, producing reliable and refined depth maps for Gaussian mean prediction.

**Iteration-based Optimization Methods.** Iteration-based optimization methods [1, 18] are widely used in various tasks [3, 13, 55] due to their ability to progressively enhance and refine the feature learning process. For instance, in optical flow estimation [14, 15, 33, 36, 48], iterative optimization is commonly used to build coarse-to-fine pyramidal features by stacking multiple feature units, resulting in more accurate and stable flow estimation. In the field of depth estimation, some works [6, 19, 37, 41, 42] have iteratively retrieved multi-view correlation features using structures like GRUs and LSTMs with shared parameters to update the disparity field, yielding better depth estimation results. Similarly, in monocular depth estimation [11, 30, 56], iterative methods are often used to gradually refine the depth search range, leading to more stable and accurate predictions. Additionally, in the 3D Gaussian Splatting (3DGS) domain,

recent methods [4, 12, 38, 45, 52] have also attempted to design iterative optimization processes to reduce the difficulty of 3D Gaussian reconstruction tasks. Unlike existing iterative optimization methods, we propose a novel Depth Probability Estimation Unit that integrates the similarity results of multiple warps in a multiplicative manner. This approach produces more reliable and refined depth maps, while progressively enhancing feature resolution and refining the depth candidate range throughout the iterative process.

### 3. Method

#### 3.1. Preliminaries.

Given a sequence of  $V$  sparse-view images  $\mathcal{I} = \{\mathbf{I}^i\}_{i=1}^V$ , where each image  $\mathbf{I}^i$  has dimensions  $H \times W \times 3$ , and the corresponding camera projection matrices are  $\mathbf{P}^i \in \mathbb{R}^{3 \times 4}$ . The goal of the generalizable 3DGS task is to learn a network that maps images to 3D Gaussian parameters. This process is defined as:

$$f_{\theta} : \{(\mathbf{I}^i, \mathbf{P}^i)\}_{i=1}^V \mapsto \{(\boldsymbol{\mu}_j, \boldsymbol{\alpha}_j, \boldsymbol{\Sigma}_j, \mathbf{c}_j)\}_{j=1}^{V \times H \times W}, \quad (1)$$

where  $f_{\theta}$  is a feed-forward network with learnable parameters  $\theta$ . The parameters  $\boldsymbol{\mu}_j$ ,  $\boldsymbol{\alpha}_j$ ,  $\boldsymbol{\Sigma}_j$ , and  $\mathbf{c}_j$  are the Gaussian mean, opacity, covariance, and color, respectively. Since Gaussian means are difficult to predict directly, most existing methods estimate them by unprojecting a depth map into 3D. The depth estimation scheme is as follows: First, the input image sequence is processed using a multi-view feature extraction backbone, resulting in a downsampled feature  $\mathbf{F} \in \mathbb{R}^{V \times \frac{H}{4} \times \frac{W}{4} \times C}$ . Then, the cost volume is computed based on  $\mathbf{F}$ , the camera projection matrices  $\mathbf{P}^i$ ,  $\mathbf{P}^j$  for different views, and the depth candidates  $\mathbf{G} = [d_1, d_2, \dots, d_D] \in \mathbb{R}^D$ . Specifically, the feature  $\mathbf{F}^j$  from view  $j$  is warped to view  $i$  as follow:

$$\mathbf{F}^{j \rightarrow i} = \mathcal{W}(\mathbf{F}^j, \mathbf{P}^i, \mathbf{P}^j, \mathbf{G}) \in \mathbb{R}^{\frac{H}{4} \times \frac{W}{4} \times D \times C}, \quad (2)$$

where  $\mathcal{W}$  denotes the warp operator. The correlation is then computed as the dot product between  $\mathbf{F}^i$  and  $\mathbf{F}_{d_m}^{j \rightarrow i}$ :

$$\mathbf{C}_{d_m}^i = (\mathbf{F}^i \cdot \mathbf{F}_{d_m}^{j \rightarrow i} / \sqrt{C}) \in \mathbb{R}^{\frac{H}{4} \times \frac{W}{4}}, \quad (3)$$

where  $m \in \{1, \dots, D\}$ . Subsequently,  $\mathbf{C}^i = [\mathbf{C}_{d_1}^i, \dots, \mathbf{C}_{d_D}^i]$  is refined with a U-Net and upsampled to the input resolution as  $\tilde{\mathbf{C}}^i \in \mathbb{R}^{H \times W \times D}$ . Finally, a softmax function is applied to obtain the probability of each candidate depth, and the final depth map is computed as their weighted average.

To achieve high-quality 3D reconstruction, an accurate depth map  $\mathbf{D}$  is crucial since it determines the centers of 3D Gaussians. However, this commonly used method only relies on a single cross-view warp to compute feature similarity, underutilizing cross-view geometry and often leading to

unstable, coarse depth estimates. In addition, this typical correlation computation method requires storing all the dense warping features, which leads to a memory issue, especially when the depth candidate size  $D$  is large.

#### 3.2. Iterative Multi-View Depth Estimation

In this paper, we propose IDESpLat to iteratively boost the feature similarity measure using multiple warp operations. As IDESpLat progressively mines geometric cues to identify high-probability potential depth candidates, it can produce refined and reliable depth probability estimation results for precise Gaussian mean prediction.

**Warp-Index Epipolar Attention.** The warp operation is key to constructing the cost volume or epipolar attention map, as it establishes pixelwise correspondences between features in the source and target views. However, as shown in Eq. (2), this warping operation requires sampling target-view features for each depth candidate, thereby incurring high memory cost. To address the inherent memory issue, we introduce a Warp-Index Epipolar Attention mechanism that only stores warp indices for similarity matrix multiplication. We first compute the warping index map  $\mathbf{I}$  as follows:

$$\mathbf{I}^{j \rightarrow i} = \mathcal{IW}(\mathbf{F}^j, \mathbf{P}^i, \mathbf{P}^j, \mathbf{G}) \in \mathbb{R}^{\frac{H}{4} \times \frac{W}{4} \times D}, \quad (4)$$

where  $\mathcal{IW}$  represents the operation that only records the indices obtained during warping, and  $\mathbf{G}$  is the depth candidate matrix. Next, we compute the feature correlations in parallel as follows:

$$\mathbf{C}^i = \Psi(\mathbf{F}^i, \mathbf{F}^{j \rightarrow i}, \mathbf{I}^{j \rightarrow i}) \in \mathbb{R}^{\frac{H}{4} \times \frac{W}{4} \times D}, \quad (5)$$

where  $\Psi$  denotes the Sparse Matrix Multiplication (SMM), which uses the warp index  $\mathbf{I}^{j \rightarrow i}$  to determine the position in  $\mathbf{F}^{j \rightarrow i}$  for matrix multiplication with  $\mathbf{F}^i$ . Then, we refine the correlation map  $\mathbf{C}^i$  with a lightweight 2D U-Net to obtain  $\tilde{\mathbf{C}}^i \in \mathbb{R}^{H \times W \times D}$ . Finally, a softmax is applied along the depth dimension to obtain the attention weights:

$$\mathbf{A}^i = \text{softmax}(\tilde{\mathbf{C}}^i). \quad (6)$$

This attention map  $\mathbf{A}^i$  corresponds to the depth probability results of view  $i$  for different depth candidates in a single estimation.

**Depth Probability Boosting Strategy.** In each depth probability boosting unit, we stack  $M$  Warp-Index Epipolar Attention layers to produce  $M$  depth probability estimation results. To combine these isolated estimated outputs for stronger depth estimation capability, we propose a depth probability boosting strategy. Specifically, we initialize the depth probability matrix as  $\mathbf{P}_0 = \mathbf{I}$  and compute the subsequent updates as follows:

$$\mathbf{P}_m = \text{Norm}(\mathbf{P}_{m-1} \odot \mathbf{A}_m), \quad (7)$$

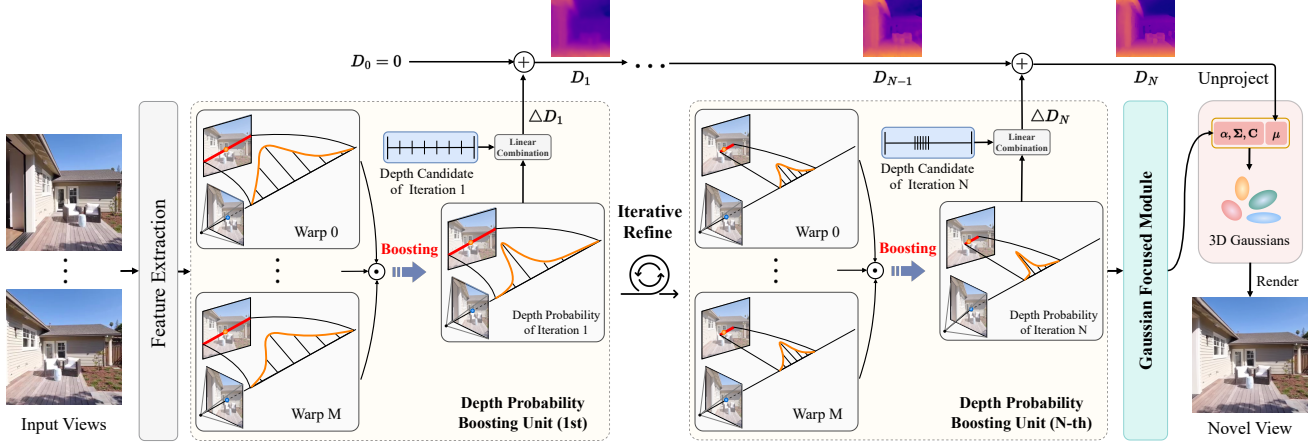


Figure 2. The overall architecture of IDESplat. IDESplat is composed of three key parts: a feature extraction backbone, an iterative depth probability estimation process, and a Gaussian Focused Module (GFM). The iterative process consists of cascaded Depth Probability Boosting Units (DPBUs). Each unit combines multi-level warp results in a multiplicative manner to mitigate the inherent instability of a single warp. As IDESplat iteratively updates the depth candidates and boosts the probability estimates, the depth map becomes more precise, leading to accurate Gaussian means.

where  $m \in \{1, \dots, M\}$  and  $\text{Norm}(\cdot)$  denotes row-wise normalization.  $\mathbf{P}_m$  represents the depth probability matrix generated by the  $m$ -th Warp-Index Epipolar Attention in the current depth probability boosting unit. Depth candidates with consistently high probabilities across layers will be boosted through this cascaded element-wise product process. As a result, the depth probability produced by the index-based epipolar attention layer can be gradually enhanced, becoming more reliable and accurate.

**Iterative Depth Estimation Process.** Based on the depth probability boosting strategy, each Depth Unit produces an enhanced depth-probability map  $\mathbf{P}_M$ . The residual depth map  $\Delta \mathbf{D}$  is then computed by linearly combining  $\mathbf{P}_M$  with the corresponding depth-candidate vector  $\mathbf{G}$ :

$$\Delta \mathbf{D} = \mathbf{P}_M \mathbf{G}, \quad (8)$$

where the combination is along the depth dimension. This residual depth  $\Delta \mathbf{D}$  is added to the previous depth estimate to obtain a refined depth map at each iteration. We initialize the depth map as  $\mathbf{D}_0 = \mathbf{0}$ , and the depth is then progressively computed in this manner:

$$\mathbf{D}_n = \mathbf{D}_{n-1} + \Delta \mathbf{D}_n, \quad (9)$$

where  $n \in \{1, \dots, N\}$ , and  $\mathbf{D}_N$  is the final depth map of the iterative depth estimation process, from which the Gaussian mean parameters are obtained through unprojection. Notably, the depth search range is updated after each depth estimation unit. The search center is determined by the previous unit’s depth estimate, and the search range is halved. Thanks to our memory-efficient Warp-Index Epipolar Attention, IDESplat can progressively increase the feature resolution throughout this iterative process. Finally, IDESplat performs warping

and similarity computation at the original input resolution of  $256 \times 256$ , producing refined depth maps.

### 3.3. Gaussian Focused Module

For the remaining Gaussian parameters, we introduce a window-based Gaussian Focused Module that can filter irrelevant Gaussians and retains the most relevant tokens for attention weight computation. The window-based attention performs pairwise interactions for each Gaussian token, often including numerous irrelevant ones. This dense interaction not only slows down the model but also introduces noise into the attention results. Inspired by [24], we introduce a Gaussian Focused Layer that reuses the previous layer’s Gaussian correlation map to guide attention in the current layer. Formally, for the Gaussian parameters of a given view,  $\mathbf{G} \in \mathbb{R}^{C \times H \times W}$ , we apply three linear layers to obtain  $\mathbf{Q}$ ,  $\mathbf{K}$ , and  $\mathbf{V}$ . We use a matrix  $\mathbf{I}_G$  to record the indices of Gaussian tokens with high similarity.  $\mathbf{I}_G^0$  is initialized as an all-one matrix and is updated after each similarity computation. Then, we compute the Gaussian similarity map as follows:

$$\mathbf{S}^l = \Psi(\mathbf{Q}^l, \mathbf{K}^l, \mathbf{I}^{l-1}), \quad (10)$$

where  $\Psi$  denotes the SMM operation, and  $\mathbf{S}^l$  is the similarity map of the  $l$ -th Gaussian-Focused Layer. Subsequently, we compute the sparse Gaussian attention map  $\mathbf{A}^l$  for the current  $l$ -th layer as follows:

$$\mathbf{A}^l = \mathcal{S}(\text{Norm}(\mathbf{A}^{l-1} \odot \text{Softmax}(\mathbf{S}^l))), \quad (11)$$

where  $\mathcal{S}$  denotes the sparsification operation that retains the top half of the weights in each row of the attention map. The positions of the retained weights are recorded as  $\mathbf{I}_G^l$ , which stores the selected highly similar Gaussian relations. Finally,

the output Gaussian features are reweighted as follows:

$$\mathbf{O}^l = \Psi(\mathbf{A}^l, \mathbf{V}^l, \mathbf{I}^l). \quad (12)$$

The Gaussian Focused Module consists of a series of Gaussian Focused Layers connected in sequence. As the layer index  $l$  increases,  $\mathbf{I}_G^l$  becomes progressively sparser, gradually identifying the Gaussian positions that are most important to each query location. This module leverages token similarity across layers to filter out the influence of irrelevant Gaussian features, achieving relational and sufficiently enriched Gaussian feature interactions.

### 3.4. Model Architecture

Our IDESpLat consists of three components: the feature extraction backbone, the iterative depth estimation process, and the gaussian focused module.

**Feature Extraction Backbone.** The feature extraction backbone follows the design of [46] and can be divided into two parts: multi-view feature extraction and monocular feature extraction. The pre-trained Unimatch [43] network is used as the multi-view feature extraction branch, and the pre-trained DepthAnything V2 [49] network based on the ViT-small version is used as the monocular feature extraction branch. The outputs of these two branches are directly stacked along the channel dimension using concatenation and then fused through convolution. This backbone captures rich multi-view geometry and texture information, which is then used as input to the iterative depth estimation process.

**Iterative Depth Estimation Process.** To achieve both high-quality reconstruction performance and real-time efficiency, we design an iterative pipeline with three Depth Probability Boosting Units (DPBUs). As a result, the pipeline produces three progressively refined depth outputs. Each DPBU consists of two Warp-Index Epipolar Attention layers connected in sequence, and their attention maps are combined via a Hadamard product to multiplicatively boost depth probabilities and yield accurate depth estimates. Across the entire pipeline, IDESpLat performs six warp operations. In addition, the feature resolution increases stage by stage—the input resolutions of the three units are  $64 \times 64$ ,  $128 \times 128$ , and  $256 \times 256$ , respectively.

**Gaussian Focused Module.** The Gaussian Focused Module consists of six Gaussian-focused layers, with a feature partition window size of 16 and a shift window strategy. After each attention calculation, sparse operations are applied to retain only the most relevant half of the Gaussian positions. The number of retained Gaussian weight values in each layer is [256, 256, 128, 128, 64, 64], respectively. The module uses multi-head attention with 6 attention heads, and the total number of channels is 256. Additionally, we incorporate LePE positional encoding [7] during the attention computation.

## 4. Experiments

### 4.1. Experiment Setting

**Datasets.** Our experiments are conducted on three large-scale datasets: RealEstate10K [54], ACID [20] and DTU [16]. RealEstate10K contains real estate videos downloaded from YouTube, which are split into 67,477 training scenes and 7,289 testing scenes. ACID consists of nature scenes captured via aerial drones, with 11,075 scenes for training and 1,972 scenes for testing. Both datasets are calibrated using the Structure-from-Motion (SfM) [29] algorithm to estimate the camera’s intrinsic and extrinsic parameters for each frame. Following the settings of previous works [2, 5, 22, 46], for the RealEstate10K and ACID datasets, two context images are used as input, and three novel target views are rendered for each test scene. All input and target images have a resolution of  $256 \times 256$ . In addition, for the multi-view DTU [16] dataset, which contains object-centric scenes with known camera poses, we report results on 16 validation scenes.

**Implementation details.** For a fair comparison, we followed the commonly used training setup [5, 22, 46]. Specifically, our training experiments were conducted on 8 RTX 4090 GPUs with a total batch size of 16, using the AdamW [25] optimizer for 300,000 iterations. We employed a cosine learning rate schedule to optimize our model. For the pre-trained Depth Anything V2 [49] backbone, we used a learning rate of  $2 \times 10^{-6}$ , while the remaining layers were trained with a learning rate of  $2 \times 10^{-4}$ .

### 4.2. Main Results

We comprehensively compare our proposed method with several leading approaches in scene-level novel view synthesis, covering three representative categories: light field network methods such as GPNR [32] and AttnRend [8]; NeRF-based methods including pixelNeRF [50] and MuRF [44]; and 3D Gaussian Splatting-based methods such as pixelSplat [2], latentSplat [39], MVSpLat [5], eFreeSplat [27], MonoSplat [22], and DepthSplat [46].

**Quantitative results.** As shown in Tab. 1, our IDESpLat achieves state-of-the-art performance on all visual quality metrics in both the RealEstate10K and ACID benchmarks. Specifically, on the RE10K dataset, compared to DepthSplat, our method improves PSNR by **0.33 dB**, while using only **10.7%** of its parameters. Additionally, compared to MonoSplat, which has a similar number of parameters, our method achieves a significant **1.12 dB** improvement. For SSIM and LPIPS metrics, our method also achieves the best results of 0.893 and 0.108, respectively. On the ACID dataset, our method achieves a **0.41 dB** improvement in PSNR over MonoSplat, reaching a maximum of **29.04 dB**. The superior performance of IDESpLat can be attributed to its iterative boosting design for depth probability prediction, which grad-

Table 1. **Quantitative comparisons.** We surpass all baseline methods in terms of PSNR, LPIPS, and SSIM for novel view synthesis on the real-world RealEstate10k [54] and ACID [20] datasets. We highlight first-place results in **bold** and second-place results with underlines in each column. ”-” Indicates that the original paper did not contain relevant data.

Method	Params (M) ↓	RealEstate10k [54]			ACID [20]		
		PSNR ↑	SSIM ↑	LPIPS ↓	PSNR ↑	SSIM ↑	LPIPS ↓
Du et al.[8]	125.1	24.78	0.820	0.213	26.88	0.799	0.218
GPNR[32]	9.6	24.11	0.793	0.255	25.28	0.764	0.332
pixelNeRF [50]	28.2	20.43	0.589	0.550	20.97	0.547	0.533
MuRF [44]	<b>5.3</b>	26.10	0.858	0.143	28.09	0.841	0.155
pixelSplat [2] (CVPR 2024)	125.4	26.09	0.863	0.136	28.27	0.843	0.146
latentSplat [39] (ECCV 2024)	187.0	23.07	0.825	0.182	24.95	0.782	0.207
MVSplat [5] (ECCV 2024)	12.0	26.39	0.869	0.128	28.25	0.843	0.144
eFreeSplat [27] (NIPS 2024)	-	26.45	0.865	0.126	28.30	0.851	0.140
MonoSplat [22] (CVPR 2025)	30.3	26.68	0.875	0.123	<u>28.63</u>	<u>0.864</u>	<u>0.138</u>
DepthSplat [46] (CVPR 2025)	354	<u>27.47</u>	<u>0.889</u>	<u>0.114</u>	-	-	-
<b>IDESplat (Ours)</b>	37.6	<b>27.80</b>	<b>0.893</b>	<b>0.107</b>	<b>29.04</b>	<b>0.866</b>	<b>0.124</b>

ually refines the depth map. This design allows our method to achieve reliable and stable depth estimation results with fewer parameters, enabling accurate Gaussian mean parameter prediction and high-quality scene reconstruction.

**Cross-Dataset Generalization.** To evaluate the generalization ability of our proposed IDESplat, we conducted cross-dataset generalization tests on unseen datasets. We first trained the model on the indoor scene dataset RealEstate10K, and then evaluated it directly on the outdoor scene ACID dataset and the object-centered DTU dataset. As shown in Tab. 2, IDESplat demonstrates outstanding cross-dataset generalization ability, outperforming existing methods on all metrics. For the DTU dataset, our method improves PSNR by **2.95 dB** over DepthSplat, and achieves the best LPIPS score of **0.239**. On the ACID dataset, our method also achieves the highest performance with **28.79 dB**. These results show that our iterative depth probability estimation method effectively enhances the modeling of cross-view feature similarity, learning strong out-of-distribution scene reconstruction capabilities. This also demonstrates that our iterative depth probability estimation method is both efficient and highly generalizable, surpassing dataset-specific features and avoiding overfitting to the training data.

**Visual comparison results.** We performed a qualitative comparison of scene reconstruction results between our method and mainstream models, including MVSplat [5], MonoSplat [22], and DepthSplat [46]. The visual comparison results are shown in Fig. 3, which include both indoor and outdoor scenes. Our proposed IDESplat achieves significantly better novel view synthesis results compared to existing mainstream open-source models. Specifically, in challenging areas with rich textures and large position and angle differences between the input images, existing methods often produce noticeable artifacts and blurring in the synthesized

Table 2. **Quantitative comparisons of cross-dataset generalization.** We perform zero-shot tests on ACID [20] and DTU [16] datasets, using models trained solely on RealEstate10K [54]. Best and second best results are **bolded** and underlined.

Method	Re10k→DTU			Re10k→ACID		
	PSNR↑	SSIM↑	LPIPS↓	PSNR↑	SSIM↑	LPIPS↓
pixelSplat [2]	12.89	0.382	0.560	27.64	0.830	0.160
MVSplat [5]	13.94	0.473	0.385	28.15	0.841	0.147
MonoSplat [22]	15.25	<u>0.605</u>	<u>0.291</u>	28.24	<u>0.848</u>	0.145
depthsplat [46]	<u>15.38</u>	0.415	0.442	<u>28.37</u>	0.847	<u>0.141</u>
<b>IDESplat (Ours)</b>	<b>18.33</b>	<b>0.719</b>	<b>0.239</b>	<b>28.79</b>	<b>0.853</b>	<b>0.135</b>

views. In contrast, IDESplat is able to generate high-quality reconstructions in these difficult regions, demonstrating excellent texture consistency and clearly showing its superiority in reconstructing complex scenes.

**Visual comparison of depth maps.** We conducted a direct qualitative comparison of depth maps predicted by IDESplat and existing state-of-the-art models, including MVSplat [5], MonoSplat [22], and DepthSplat [46]. It is important to note that the generalizable 3DGS task typically does not have depth ground truth, so we analyzed the results using the corresponding reference RGB images as input. As shown in Fig. 4, our proposed IDESplat method consistently outperforms existing methods in both indoor and outdoor scenes. Even in areas where the foreground and background are highly similar or in regions with rich texture details, our method can clearly distinguish objects at different depths. Additionally, the depth estimation results of IDESplat exhibit better and more realistic depth effects, with finer texture details, in both indoor and outdoor scenes. This is because our method can integrate the results of feature similarity from multiple warps using the depth probability boosting strat-

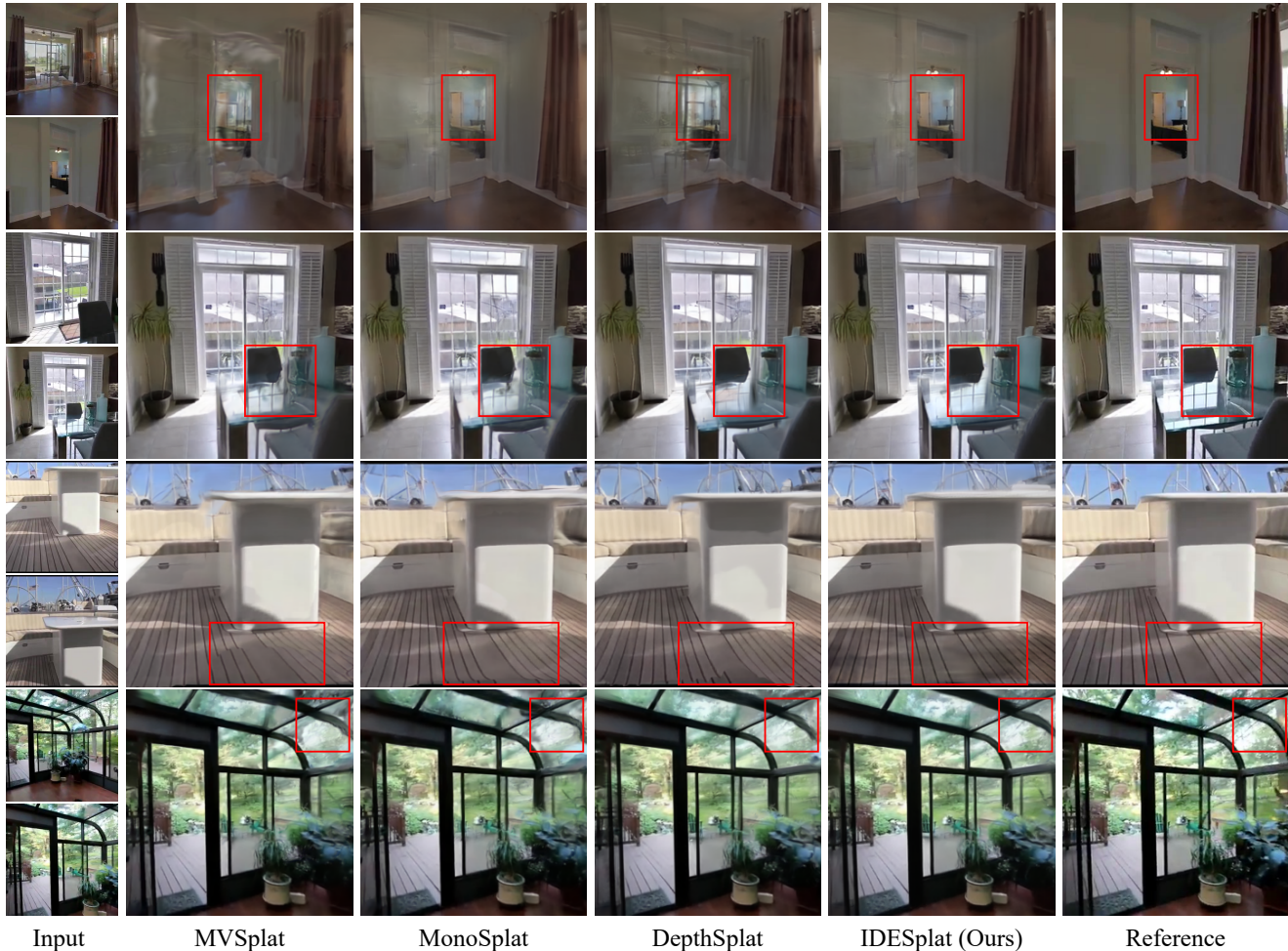


Figure 3. The comparison of visualization results for novel view synthesis on the RealEstate10K dataset. Our IDESplat significantly outperforms previous state-of-the-art methods in rendering challenging regions.

egy, enabling more accurate depth estimation. Furthermore, by performing warp calculations at the original scale, our method captures and utilizes fine textures in the image, leading to more detailed and precise predictions. More visual results can be found in the supplementary materials.

**Comparison of model efficiency.** In Tab. 3, we compare the model efficiency of IDESplat with several classic methods, including PixelSplat, MVSplat, and the latest methods such as MonoSplat and DepthSplat. We measure inference time and memory usage with two-view inputs at a resolution of  $256 \times 256$ , and the PSNR values are reported on the commonly used benchmark dataset RE10K. Although our method shows slightly lower inference efficiency compared to DepthSplat, it outperforms DepthSplat on all other metrics. Despite using significantly fewer parameters and computational resources than DepthSplat, IDESplat achieves better results. The superior performance of IDESplat with fewer parameters and better memory efficiency is due to our iterative depth probability estimation architecture, which

Table 3. **Comparison of model efficiency.** Our method demonstrates relatively low inference costs and reduced memory usage.

Method	Params (M)	Mem. (M)	Time (s)	PSNR $\uparrow$
pixelSplat [2]	125.4	4108	0.120	26.09
MVSplat [5]	<b>12.0</b>	1940	<b>0.054</b>	26.39
MonoSplat [22]	30.3	<b>1606</b>	0.062	26.68
depthsplat [46]	354	3342	0.082	27.47
<b>IDESplat (Ours)</b>	37.6	2336	0.110	<b>27.80</b>

performs multiple warp operations to improve the accuracy of Gaussian mean parameter predictions.

### 4.3. Ablation Study

We conducted detailed ablation experiments on various components of the proposed IDESplat. All models were trained for 20,000 iterations on the RealEstate10K dataset with a batch size of 8. We analyzed the effectiveness of the gaussian focused module (GFM), iterative depth Estimation process (IDE), and depth probability boosting strategy (DPBS),

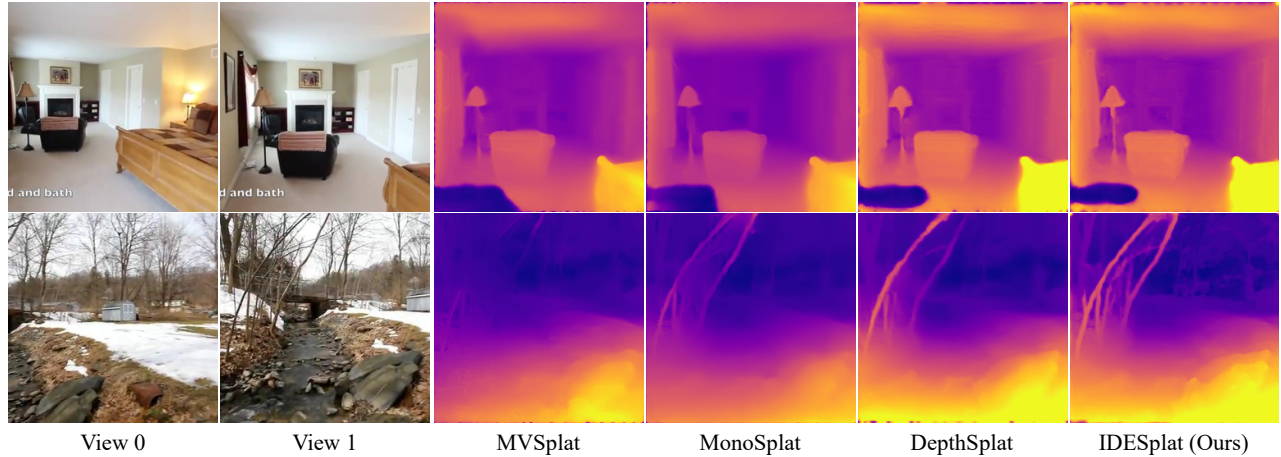


Figure 4. Comparison of depth prediction maps for different models on the RE10K dataset.

Table 4. **Ablation study results for each component of IDESplat.** All results are reported on the RealEstate10K dataset. GFM denotes the Gaussian Focused Module, IDE(3) denotes the Iterative Depth Estimation process with three iterations, and DPBS denotes the Depth Probability Boosting Strategy.

Method	PSNR $\uparrow$	SSIM $\uparrow$	LPIPS $\downarrow$
Baseline	26.31	0.866	0.129
+ GFM	26.63	0.875	0.124
+ IDE(3)	26.88	0.878	0.120
+ IDE(3) + GFM	27.07	0.882	0.118
+ IDE(3) + DPBS	27.34	0.887	0.112
Full Model	<b>27.56</b>	<b>0.889</b>	<b>0.110</b>

while keeping all other training settings consistent. It should be noted that IDE(3) indicates the model iterates the depth probability boosting unit three times. The detailed experimental results, shown in Tab. 4, demonstrate that all three designs contribute to improved reconstruction performance. Specifically, adding GFM and IDE(3) results in improvements of 0.32 dB and 0.57 dB, respectively, showing that both the iterative depth estimation process and the Gaussian focused module effectively enhance scene reconstruction. The performance improves significantly by 0.46 dB when we incorporate the DPBS strategy into the iterative process, and the best result of 27.56 dB is achieved when all three strategies are used together, further validating the effectiveness of our proposed method.

To comprehensively analyze the efficiency and reconstruction performance of IDESplat with different iteration counts, we conducted detailed ablation experiments. In these experiments, the Gaussian Focused Module and Depth Probability Boosting Strategy were used by default. Additionally, during the iterative process, we gradually increased the resolution, and the depth search range was progressively halved. For 3

Table 5. **Ablation results for IDESplat with different numbers of iterative depth probability boosting units.** All results are reported on the RealEstate10K dataset. Here, an iteration count of 0 denotes using a single warp operation without any DPBUs, while the other entries correspond to using different numbers of DPBUs.

Iterations	Params (M)	Mem. (M)	Time (s)	PSNR $\uparrow$	SSIM $\uparrow$	LPIPS $\downarrow$
0	35.4	1674	0.056	26.63	0.875	0.124
1	36.8	1734	0.071	27.08	0.882	0.113
2	37.3	1902	0.091	27.31	0.884	0.112
3	37.6	2336	0.110	27.56	0.889	0.110
4	38.0	2745	0.132	27.64	0.890	0.109

iterations, the feature resolutions during warping were  $\frac{1}{4}$ ,  $\frac{1}{2}$ , and 1 of the original resolution. For 4 iterations, the model iterates twice at the largest feature size. When the number of iterations is 0, it represents performing a single warp for depth probability estimation. The results of the experiment, as shown in Tab. 5, indicate that even with a single iteration, our method provides a 0.45 dB improvement. With 3 iterations, the performance improves by 0.93 dB. Furthermore, as the number of iterations increases, the increase in parameters is minimal, and the memory usage remains comparable to existing methods. Although inference time increases with more iterations, the performance improvement is substantial by the third iteration, while still maintaining real-time inference.

## 5. Conclusion

We propose IDESplat, which iteratively applies warp operations and integrates multi-level epipolar attention maps to enhance depth probability estimation for accurate Gaussian mean prediction. Specifically, we first design a depth probability boosting unit to amplify cross-view feature similarity in a multiplicative manner. Then, we build an iterative depth estimation process by stacking multiple DPBUs, gradually identifying the most likely

depth locations. Additionally, during this iterative process, we progressively narrow the depth search range and increase feature size to achieve more precise depth estimates. For the other Gaussian parameters, we design a gaussian focused module to select the most relevant Gaussian tokens for attention-based feature interaction. Experimental results on large-scale benchmarks clearly show that IDEsplat achieves excellent reconstruction quality and strong domain generalization ability. Our current model still has limitations: although it enables real-time 3D reconstruction, its efficiency could be further improved, and it requires camera pose input as a prerequisite. Potential directions for improvement include further enhancing inference speed and exploring a pose-free framework.

## References

- [1] Jonas Adler and Ozan Öktem. Solving ill-posed inverse problems using iterative deep neural networks. *Inverse Problems*, 33(12):124007, 2017. 2
- [2] David Charatan, Sizhe Lester Li, Andrea Tagliasacchi, and Vincent Sitzmann. pixelsplat: 3d gaussian splats from image pairs for scalable generalizable 3d reconstruction. In *Proceedings of the IEEE/CVF conference on computer vision and pattern recognition*, pages 19457–19467, 2024. 1, 2, 5, 6, 7
- [3] Changrui Chen, Jungong Han, and Kurt Debattista. Virtual category learning: A semi-supervised learning method for dense prediction with extremely limited labels. *IEEE transactions on pattern analysis and machine intelligence*, 46(8): 5595–5611, 2024. 2
- [4] Yun Chen, Jingkang Wang, Ze Yang, Sivabalan Manivasagam, and Raquel Urtasun. G3r: Gradient guided generalizable reconstruction. In *European Conference on Computer Vision*, pages 305–323. Springer, 2024. 3
- [5] Yuedong Chen, Haofei Xu, Chuanxia Zheng, Bohan Zhuang, Marc Pollefeys, Andreas Geiger, Tat-Jen Cham, and Jianfei Cai. Mvsplat: Efficient 3d gaussian splatting from sparse multi-view images. In *European Conference on Computer Vision*, pages 370–386. Springer, 2024. 1, 2, 5, 6, 7
- [6] Ziyang Chen, Wei Long, He Yao, Yongjun Zhang, Bingshu Wang, Yongbin Qin, and Jia Wu. Mocha-stereo: Motif channel attention network for stereo matching. In *Proceedings of the IEEE/CVF conference on computer vision and pattern recognition*, pages 27768–27777, 2024. 2
- [7] Xiaoyi Dong, Jianmin Bao, Dongdong Chen, Weiming Zhang, Nenghai Yu, Lu Yuan, Dong Chen, and Baining Guo. Cswin transformer: A general vision transformer backbone with cross-shaped windows. In *Proceedings of the IEEE/CVF conference on computer vision and pattern recognition*, pages 12124–12134, 2022. 5
- [8] Yilun Du, Cameron Smith, Ayush Tewari, and Vincent Sitzmann. Learning to render novel views from wide-baseline stereo pairs. In *CVPR*, 2023. 5, 6
- [9] Zhiwen Fan, Wenyan Cong, Kairun Wen, Kevin Wang, Jian Zhang, Xinghao Ding, Danfei Xu, Boris Ivanovic, Marco Pavone, Georgios Pavlakos, et al. Instantsplat: Sparse-view gaussian splatting in seconds. *arXiv preprint arXiv:2403.20309*, 2024. 2
- [10] Guofeng Feng, Siyan Chen, Rong Fu, Zimu Liao, Yi Wang, Tao Liu, Boni Hu, Linning Xu, Zhilin Pei, Hengjie Li, et al. Flashgs: Efficient 3d gaussian splatting for large-scale and high-resolution rendering. In *Proceedings of the Computer Vision and Pattern Recognition Conference*, pages 26652–26662, 2025. 2
- [11] Huan Fu, Mingming Gong, Chaohui Wang, Kayhan Batmanghelich, and Dacheng Tao. Deep ordinal regression network for monocular depth estimation. In *Proceedings of the IEEE conference on computer vision and pattern recognition*, pages 2002–2011, 2018. 2
- [12] James Harrison, Luke Metz, and Jascha Sohl-Dickstein. A closer look at learned optimization: Stability, robustness, and inductive biases. *Advances in neural information processing systems*, 35:3758–3773, 2022. 3
- [13] Jing He, Haodong Li, Wei Yin, Yixun Liang, Leheng Li, Kaiqiang Zhou, Hongbo Zhang, Bingbing Liu, and Ying-Cong Chen. Lotus: Diffusion-based visual foundation model for high-quality dense prediction. *arXiv preprint arXiv:2409.18124*, 2024. 2
- [14] Tak-Wai Hui, Xiaoou Tang, and Chen Change Loy. Lite-flownet: A lightweight convolutional neural network for optical flow estimation. In *Proceedings of the IEEE conference on computer vision and pattern recognition*, pages 8981–8989, 2018. 2
- [15] Eddy Ilg, Nikolaus Mayer, Tonmoy Saikia, Margret Keuper, Alexey Dosovitskiy, and Thomas Brox. Flownet 2.0: Evolution of optical flow estimation with deep networks. In *Proceedings of the IEEE conference on computer vision and pattern recognition*, pages 2462–2470, 2017. 2
- [16] Rasmus Jensen, Anders Dahl, George Vogiatzis, Engin Tola, and Henrik Aanæs. Large scale multi-view stereopsis evaluation. In *CVPR*, 2014. 5, 6
- [17] Bernhard Kerbl, Georgios Kopanas, Thomas Leimkühler, and George Drettakis. 3d gaussian splatting for real-time radiance field rendering. *ACM Trans. Graph.*, 42(4):139–1, 2023. 1, 2
- [18] Yi Li, Gu Wang, Xiangyang Ji, Yu Xiang, and Dieter Fox. Deepim: Deep iterative matching for 6d pose estimation. In *Proceedings of the European conference on computer vision (ECCV)*, pages 683–698, 2018. 2
- [19] Lahav Lipson, Zachary Teed, and Jia Deng. Raft-stereo: Multilevel recurrent field transforms for stereo matching. In *2021 International Conference on 3D Vision (3DV)*, pages 218–227. IEEE, 2021. 2
- [20] Andrew Liu, Richard Tucker, Varun Jampani, Ameesh Makadia, Noah Snavely, and Angjoo Kanazawa. Infinite nature: Perpetual view generation of natural scenes from a single image. In *ICCV*, 2021. 5, 6
- [21] Tianqi Liu, Guangcong Wang, Shoukang Hu, Liao Shen, Xinyi Ye, Yuhang Zang, Zhiguo Cao, Wei Li, and Ziwei Liu. Mvs gaussian: Fast generalizable gaussian splatting reconstruction from multi-view stereo. In *European Conference on Computer Vision*, pages 37–53. Springer, 2024. 1, 2
- [22] Yifan Liu, Keyu Fan, Weihao Yu, Chenxin Li, Hao Lu, and Yixuan Yuan. Monosplat: Generalizable 3d gaussian splatting

- from monocular depth foundation models. In *Proceedings of the Computer Vision and Pattern Recognition Conference*, pages 21570–21579, 2025. 1, 2, 5, 6, 7
- [23] Stephen Lombardi, Tomas Simon, Jason Saragih, Gabriel Schwartz, Andreas Lehrmann, and Yaser Sheikh. Neural volumes: Learning dynamic renderable volumes from images. *arXiv preprint arXiv:1906.07751*, 2019. 2
- [24] Wei Long, Xingyu Zhou, Leheng Zhang, and Shuhang Gu. Progressive focused transformer for single image super-resolution. In *Proceedings of the Computer Vision and Pattern Recognition Conference*, pages 2279–2288, 2025. 4
- [25] Ilya Loshchilov and Frank Hutter. Decoupled weight decay regularization. *arXiv preprint arXiv:1711.05101*, 2017. 5, 1
- [26] Ben Mildenhall, Pratul P Srinivasan, Matthew Tancik, Jonathan T Barron, Ravi Ramamoorthi, and Ren Ng. Nerf: Representing scenes as neural radiance fields for view synthesis. *Communications of the ACM*, 65(1):99–106, 2021. 2
- [27] Zhiyuan Min, Yawei Luo, Jianwen Sun, and Yi Yang. Epipolar-free 3d gaussian splatting for generalizable novel view synthesis. *arXiv preprint arXiv:2410.22817*, 2024. 5, 6
- [28] Michael Niemeyer, Fabian Manhardt, Marie-Julie Rakotosaona, Michael Oechsle, Daniel Duckworth, Rama Gosula, Keisuke Tateno, John Bates, Dominik Kaeser, and Federico Tombari. Radsplat: Radiance field-informed gaussian splatting for robust real-time rendering with 900+ fps. In *2025 International Conference on 3D Vision (3DV)*, pages 134–144. IEEE, 2025. 2
- [29] Johannes L Schonberger and Jan-Michael Frahm. Structure-from-motion revisited. In *Proceedings of the IEEE conference on computer vision and pattern recognition*, pages 4104–4113, 2016. 5
- [30] Shuwei Shao, Zhongcai Pei, Xingming Wu, Zhong Liu, Weihai Chen, and Zhengguo Li. Iebins: Iterative elastic bins for monocular depth estimation. *Advances in Neural Information Processing Systems*, 36:53025–53037, 2023. 2
- [31] Vincent Sitzmann, Julien Martel, Alexander Bergman, David Lindell, and Gordon Wetzstein. Implicit neural representations with periodic activation functions. *Advances in neural information processing systems*, 33:7462–7473, 2020. 2
- [32] Mohammed Suhail, Carlos Esteves, Leonid Sigal, and Ameesh Makadia. Generalizable patch-based neural rendering. In *ECCV*, 2022. 5, 6
- [33] Deqing Sun, Xiaodong Yang, Ming-Yu Liu, and Jan Kautz. Pwc-net: Cnns for optical flow using pyramid, warping, and cost volume. In *Proceedings of the IEEE conference on computer vision and pattern recognition*, pages 8934–8943, 2018. 2
- [34] Stanislaw Szymanowicz, Christian Rupprecht, and Andrea Vedaldi. Splatter image: Ultra-fast single-view 3d reconstruction. In *Proceedings of the IEEE/CVF conference on computer vision and pattern recognition*, pages 10208–10217, 2024. 2
- [35] Shengji Tang, Weicai Ye, Peng Ye, Weihao Lin, Yang Zhou, Tao Chen, and Wanli Ouyang. Hisplat: Hierarchical 3d gaussian splatting for generalizable sparse-view reconstruction. *arXiv preprint arXiv:2410.06245*, 2024. 2
- [36] Zachary Teed and Jia Deng. Raft: Recurrent all-pairs field transforms for optical flow. In *European conference on computer vision*, pages 402–419. Springer, 2020. 2
- [37] Fangjinhua Wang, Silvano Galliani, Christoph Vogel, and Marc Pollefeys. Itermvts: Iterative probability estimation for efficient multi-view stereo. In *Proceedings of the IEEE/CVF conference on computer vision and pattern recognition*, pages 8606–8615, 2022. 2
- [38] Jing Wen, Alex Schwing, and Shenlong Wang. Life-gom: Generalizable human rendering with learned iterative feedback over multi-resolution gaussians-on-mesh. In *The Thirteenth International Conference on Learning Representations*. 3
- [39] Christopher Wewer, Kevin Raj, Eddy Ilg, Bernt Schiele, and Jan Eric Lenssen. latentsplat: Autoencoding variational gaussians for fast generalizable 3d reconstruction. *arXiv preprint arXiv:2403.16292*, 2024. 5, 6
- [40] Yiheng Xie, Towaki Takikawa, Shunsuke Saito, Or Litany, Shiqin Yan, Numair Khan, Federico Tombari, James Tompkin, Vincent Sitzmann, and Srinath Sridhar. Neural fields in visual computing and beyond. In *Computer graphics forum*, pages 641–676. Wiley Online Library, 2022. 2
- [41] Gangwei Xu, Xianqi Wang, Xiaohuan Ding, and Xin Yang. Iterative geometry encoding volume for stereo matching. In *Proceedings of the IEEE/CVF conference on computer vision and pattern recognition*, pages 21919–21928, 2023. 2
- [42] Gangwei Xu, Xianqi Wang, Zhaoxing Zhang, Junda Cheng, Chunyuan Liao, and Xin Yang. Igev++: Iterative multi-range geometry encoding volumes for stereo matching. *IEEE Transactions on Pattern Analysis and Machine Intelligence*, 2025. 2
- [43] Haofei Xu, Jing Zhang, Jianfei Cai, Hamid Rezatofighi, Fisher Yu, Dacheng Tao, and Andreas Geiger. Unifying flow, stereo and depth estimation. *IEEE Transactions on Pattern Analysis and Machine Intelligence*, 45(11):13941–13958, 2023. 5, 1
- [44] Haofei Xu, Anpei Chen, Yuedong Chen, Christos Sakaridis, Yulun Zhang, Marc Pollefeys, Andreas Geiger, and Fisher Yu. Murf: Multi-baseline radiance fields. In *CVPR*, 2024. 5, 6
- [45] Haofei Xu, Daniel Barath, Andreas Geiger, and Marc Pollefeys. Resplat: Learning recurrent gaussian splats. *arXiv preprint arXiv:2510.08575*, 2025. 3
- [46] Haofei Xu, Songyou Peng, Fangjinhua Wang, Hermann Blum, Daniel Barath, Andreas Geiger, and Marc Pollefeys. Depth-splat: Connecting gaussian splatting and depth. In *Proceedings of the Computer Vision and Pattern Recognition Conference*, pages 16453–16463, 2025. 1, 2, 5, 6, 7
- [47] Yunzhi Yan, Haotong Lin, Chenxu Zhou, Weijie Wang, Haiyang Sun, Kun Zhan, Xianpeng Lang, Xiaowei Zhou, and Sida Peng. Street gaussians: Modeling dynamic urban scenes with gaussian splatting. In *European Conference on Computer Vision*, pages 156–173. Springer, 2024. 2
- [48] Gengshan Yang and Deva Ramanan. Volumetric correspondence networks for optical flow. *Advances in neural information processing systems*, 32, 2019. 2
- [49] Lihe Yang, Bingyi Kang, Zilong Huang, Zhen Zhao, Xiao-gang Xu, Jiashi Feng, and Hengshuang Zhao. Depth anything

- v2. *Advances in Neural Information Processing Systems*, 37: 21875–21911, 2024. 5, 1
- [50] Alex Yu, Vickie Ye, Matthew Tancik, and Angjoo Kanazawa. pixelnerf: Neural radiance fields from one or few images. In *Proceedings of the IEEE/CVF conference on computer vision and pattern recognition*, pages 4578–4587, 2021. 5, 6
- [51] Zehao Yu, Anpei Chen, Binbin Huang, Torsten Sattler, and Andreas Geiger. Mip-splatting: Alias-free 3d gaussian splatting. In *Proceedings of the IEEE/CVF conference on computer vision and pattern recognition*, pages 19447–19456, 2024. 1
- [52] Chuanrui Zhang, Yingshuang Zou, Zhuoling Li, Minmin Yi, and Haoqian Wang. Transplat: Generalizable 3d gaussian splatting from sparse multi-view images with transformers. In *Proceedings of the AAAI Conference on Artificial Intelligence*, pages 9869–9877, 2025. 1, 3
- [53] Shengjun Zhang, Xin Fei, Fangfu Liu, Haixu Song, and Yueqi Duan. Gaussian graph network: Learning efficient and generalizable gaussian representations from multi-view images. *Advances in Neural Information Processing Systems*, 37:50361–50380, 2024. 1
- [54] Tinghui Zhou, Richard Tucker, John Flynn, Graham Fyffe, and Noah Snavely. Stereo magnification: learning view synthesis using multiplane images. *TOG*, page 65, 2018. 5, 6
- [55] Lanyun Zhu, Tianrun Chen, Jianxiong Yin, Simon See, and Jun Liu. Addressing background context bias in few-shot segmentation through iterative modulation. In *Proceedings of the IEEE/CVF conference on computer vision and pattern recognition*, pages 3370–3379, 2024. 2
- [56] Yiming Zuo and Jia Deng. Ogni-dc: Robust depth completion with optimization-guided neural iterations. In *European Conference on Computer Vision*, pages 78–95. Springer, 2024. 2

# IDESplat: Iterative Depth Probability Estimation for Generalizable 3D Gaussian Splatting

## Supplementary Material

In this supplementary material, we provide additional details on model training, model architecture, ablation study on DPBU, experimental results on the DL3DV dataset, and more visual comparison results. Specifically, in Section A, we present the training details of the IDESplat model. In Section B, we provide the model architecture details of IDESplat and Warp-Index Epipolar Attention. In Section C, we present the experimental results of IDESplat on the DL3DV dataset, along with the ablation study on Depth Probability Boosting Units. Finally, in Section D, we include more visual comparison results for novel view synthesis and depth prediction.

### A. Training Details

For a fair comparison, we trained our IDESplat using a standard setup [5, 22, 46]. The training was done on 8 RTX 4090 GPUs with a batch size of 16, using the AdamW [25] optimizer for 300,000 iterations, taking almost 3 days. We used a cosine learning rate schedule. For the pre-trained Depth Anything V2 [49] backbone, the learning rate was  $2 \times 10^{-6}$ , while other layers were trained with a learning rate of  $2 \times 10^{-4}$ . The network was trained with a combination of MSE and LPIPS losses between the rendered and ground truth images. Following [46], for the newly added DL3DV dataset, we trained at a resolution of  $256 \times 448$ . First, we pre-trained on re10k and then fine-tuned on the DL3DV dataset for 100K iterations, with a total batch size of 4, and the number of input views was randomly sampled from 2 to 6. During inference, we evaluated the model’s performance on different numbers of input views.

### B. Model Architecture Details

We provide a detailed description of the IDESplat network architecture, as shown in Figure 5. It consists of three main parts: a feature extraction backbone, an iterative depth estimation process, and a Gaussian focus module. The backbone has two branches: a multi-view branch using the pre-trained Unimatch [43] and a monocular branch using the ViT-small version of DepthAnything V2 [49]. The outputs from both branches are fused to provide multi-view geometry and texture information for the next modules. The depth estimation process includes three Depth Probability Boosting Units (DPBU) that sequentially generate optimized depth results. Each DPBU contains two cascaded Warp-Index Epipolar Attention layers, which use the Hadamard product to enhance depth probabilities. The process is repeated for six

transformations at resolutions of  $64 \times 64$ ,  $128 \times 128$ , and  $256 \times 256$ . The GFM has six layers, using a shifting window strategy with a window size of 16. After each attention calculation, the top half of the most relevant Gaussian positions are retained. The number of retained Gaussian weights per layer is [256, 256, 128, 128, 64, 64], and the module uses 6 attention heads with 256 channels in total.

To address the memory issues in existing warp computations for cross-view similarity, we introduce Warp-Index Epipolar Attention. Unlike the existing method, which samples target view features for each depth candidate and consumes a lot of memory, our approach only stores transformation indices for similarity matrix multiplication and uses Sparse Matrix Multiplication (SMM) for efficient computation. This design enables IDESplat to perform multiple rounds of warp and depth estimation more efficiently.

### C. More Experimental Results

We conducted additional experiments on the DL3DV dataset to further evaluate the proposed IDESplat method. DL3DV is a large-scale real-world multi-view video dataset, which helps validate our method’s reconstruction capability in more complex and larger scenes. The experimental results, shown in Table 6, demonstrate outstanding performance of our method compared to existing MV-Splat and DepthSplat methods. IDESplat outperforms DepthSplat by **0.62dB**, **0.41dB**, and **0.42dB** when using 2, 4, and 6 input views, respectively. These results clearly show that our IDESplat provides better reconstruction performance in large, complex scenes with multiple input views compared to existing methods.

We also conducted ablation experiments on DPBU with different numbers of Warp-Index Epipolar Attention. The results in Table 7 show that depth probabilities can only undergo Multiplicative Boosting when more than one Warp-Index Epipolar Attention is used. Our IDESplat performs well when the number of attention layers exceeds one, and the performance improves as the number of layers increases. Considering both efficiency and performance, we chose the model with two Warp-Index Epipolar Attention layers.

### D. More Visual Comparison Results

We also provide more visual comparison results in this supplementary material, as shown in Fig. 7 and Fig. 8. Through these qualitative visual comparisons, it can be observed that our IDESplat outperforms existing methods in novel view synthesis. Even in complex lighting and textured regions, our

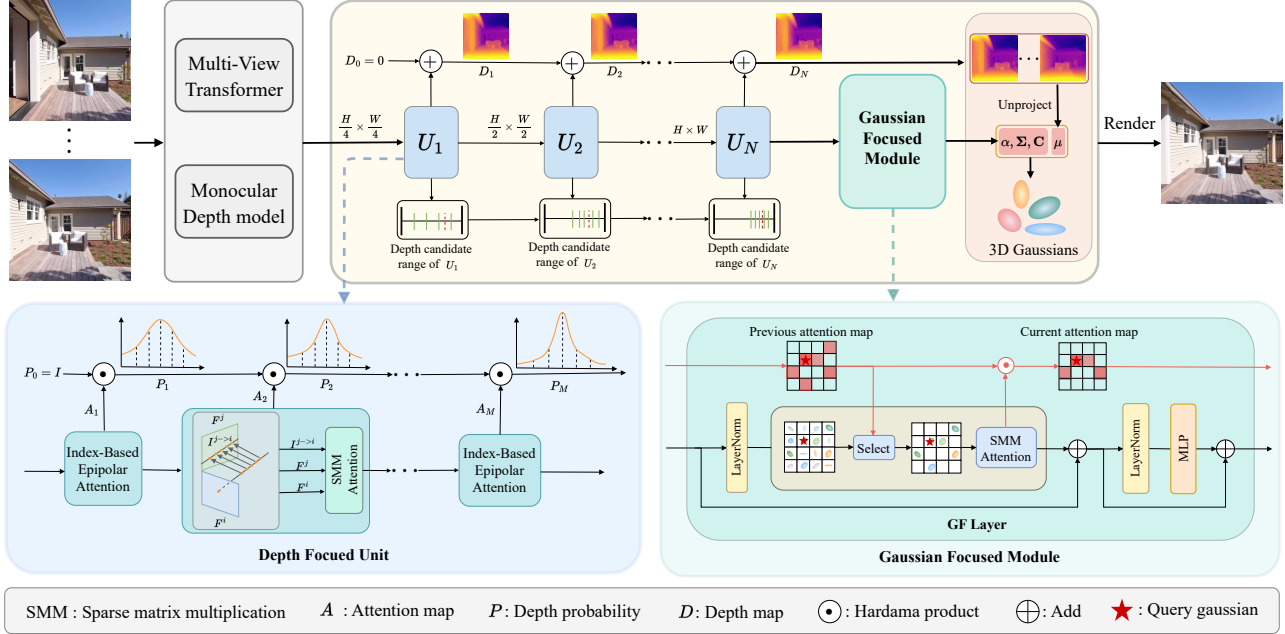


Figure 5. The architecture of IDESpLat. IDESpLat comprises a feature extraction backbone, an iterative depth estimation process with cascaded Depth Probability Boosting Units (DPBUs), and a Gaussian Focused Module (GFM).

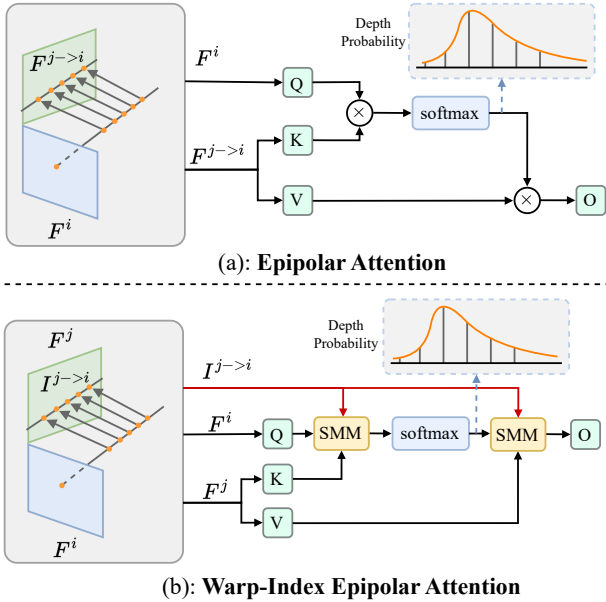


Figure 6. The difference between Warp-Index Epipolar Attention and Epipolar Attention.

method achieves better reconstruction results. Furthermore, in Fig. 9 and Fig. 10, we provide more qualitative depth map comparisons. The results show that our method significantly improves both the consistency and fine texture details of the depth maps, whether in indoor or outdoor environments, compared to existing methods. To show how IDESpLat refines depth maps over iterations, we compare results visually

Table 6. **Quantitative Experimental Results and Comparisons on DL3DV.** Our IDESpLat consistently outperforms MVSpLat and DepthSpLat across different numbers of input views.

Method	#Views	PSNR $\uparrow$	SSIM $\uparrow$	LPIPS $\downarrow$
MVSpLat [5]	2	17.54	0.529	0.402
DepthSpLat [46]		19.31	0.615	0.310
IDESpLat		<b>19.93</b>	<b>0.635</b>	<b>0.300</b>
MVSpLat [5]	4	21.63	0.721	0.233
DepthSpLat [46]		23.12	0.780	0.178
IDESpLat		<b>23.53</b>	<b>0.789</b>	<b>0.176</b>
MVSpLat [5]	6	22.93	0.775	0.193
DepthSpLat [46]		24.19	0.823	0.147
IDESpLat		<b>24.61</b>	<b>0.829</b>	<b>0.146</b>

Table 7. **Ablation results for DPBU with different numbers of Warp-Index Epipolar Attention.** All results are reported on the RealEstate10K dataset.

Number of WIEA	Params (M)	Mem. (M)	Time (s)	PSNR $\uparrow$	SSIM $\uparrow$	LPIPS $\downarrow$
1	36.4	2033	0.082	27.11	0.882	0.116
2	37.6	2336	0.110	27.56	0.889	0.110
3	38.9	2642	0.139	27.65	0.890	0.109
4	40.2	2954	0.172	27.72	0.893	0.107

in Fig. 11. Each iteration represents one pass through the Depth Probability Boosting Unit. We can see that with more steps, the depth map gets better and more detailed. After 3 steps, the model can work at the original image size and the depth map is clearer. With more iterations, the depth map improves. This leads to more accurate Gaussian centers, which creates a better scene reconstruction.

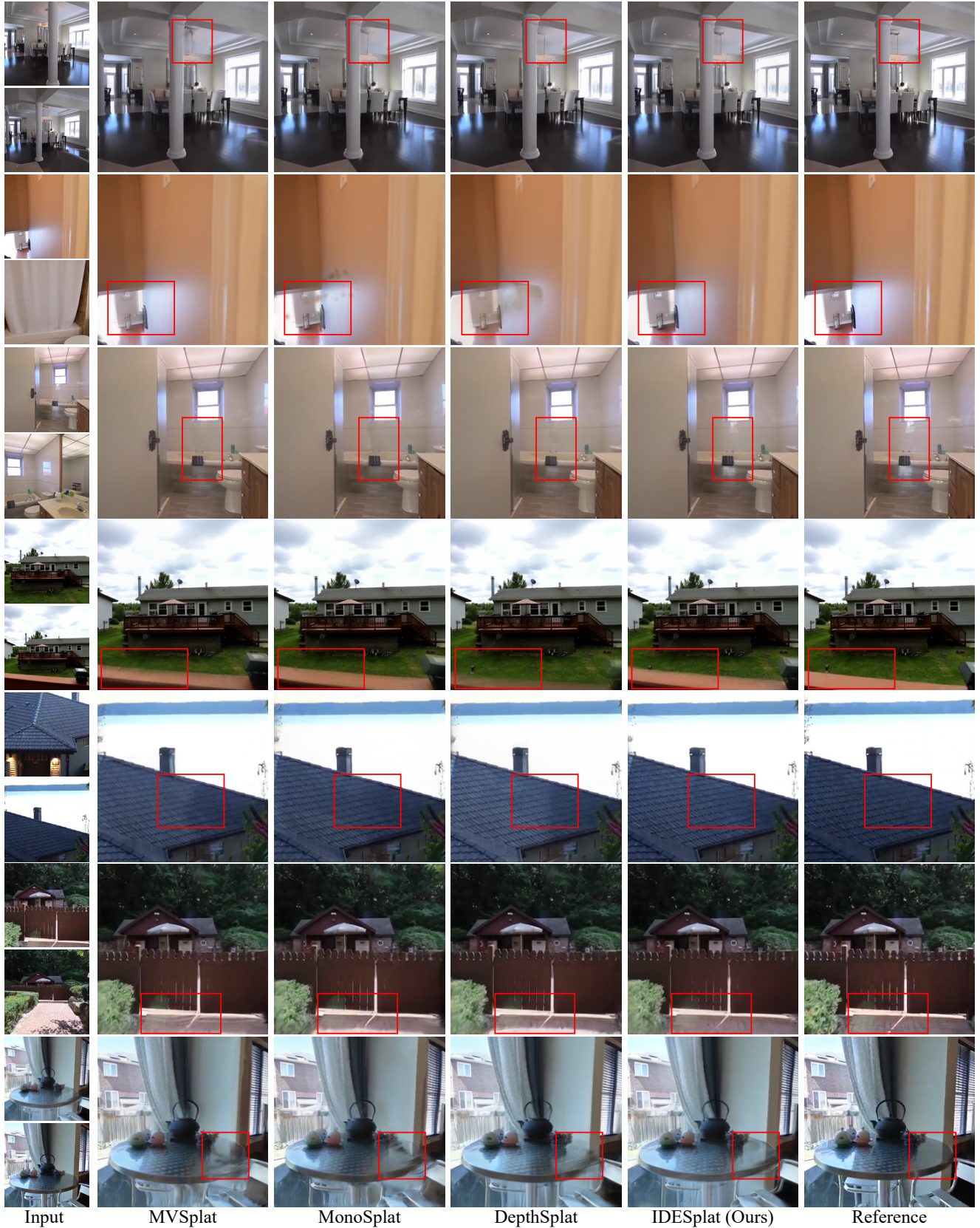
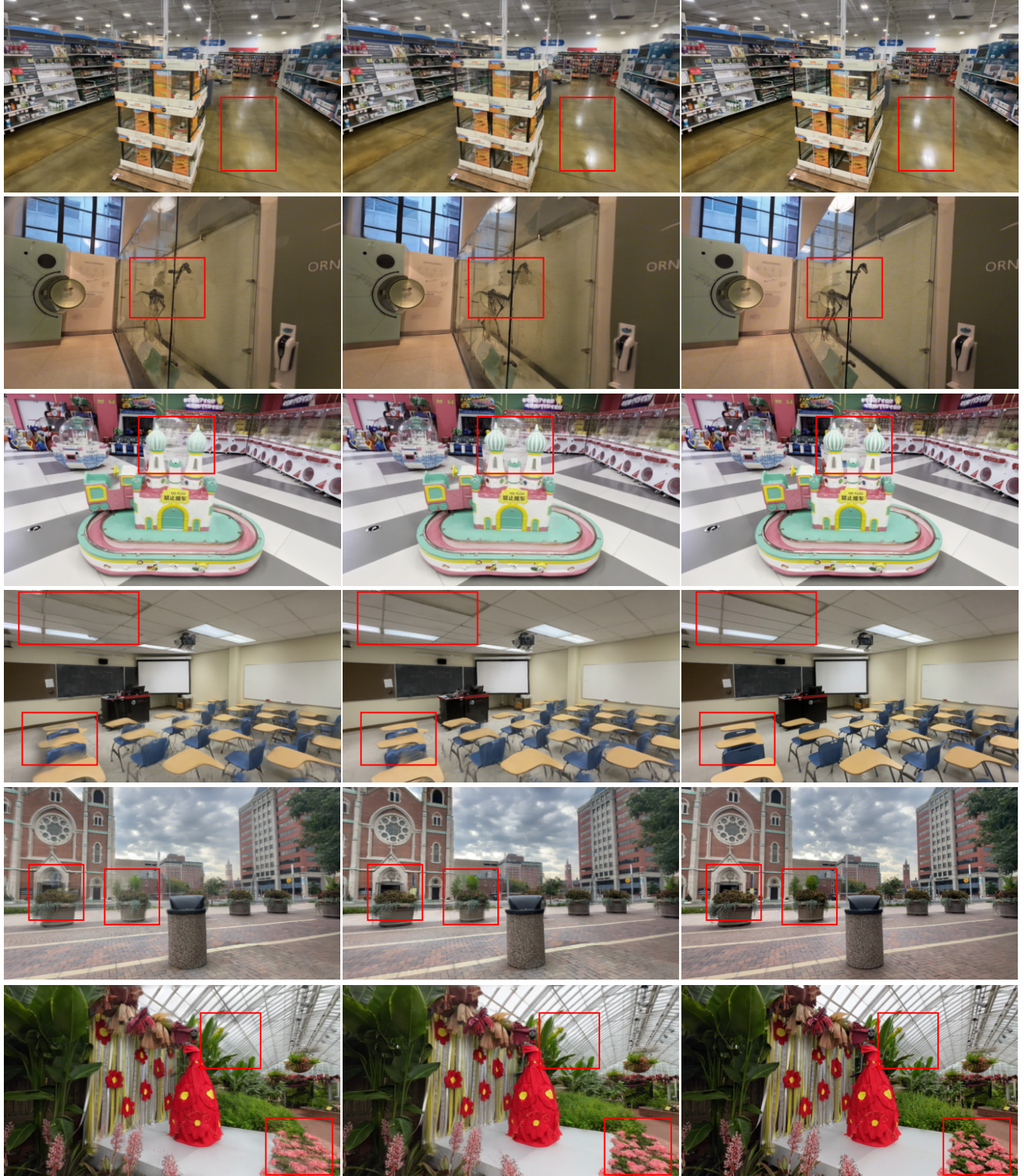


Figure 7. The comparison of visualization results for novel view synthesis on the RealEstate10K dataset.



DepthSplat

IDESplat (Ours)

Reference

Figure 8. The comparison of visualization results for novel view synthesis on the DL3DV dataset.

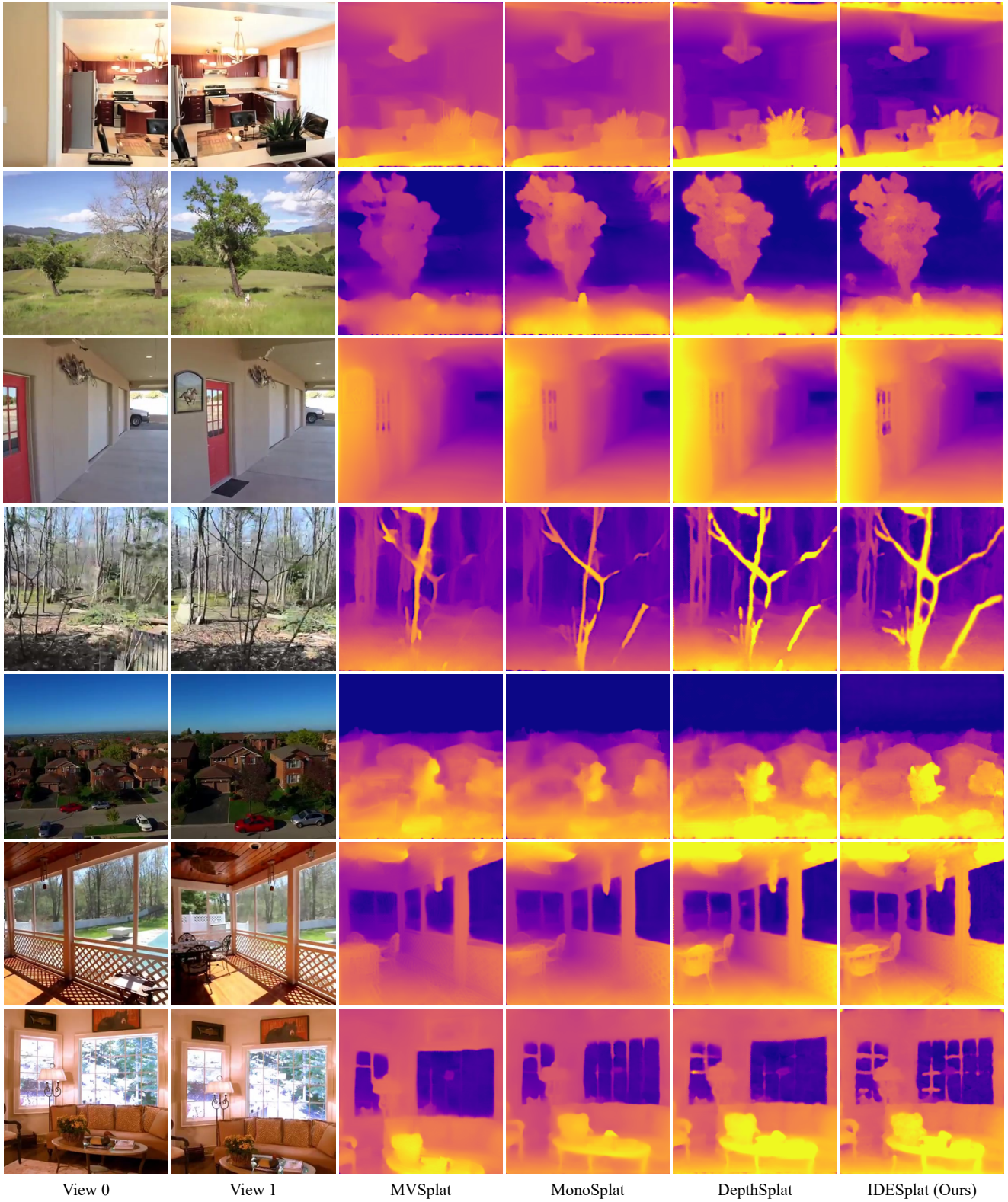
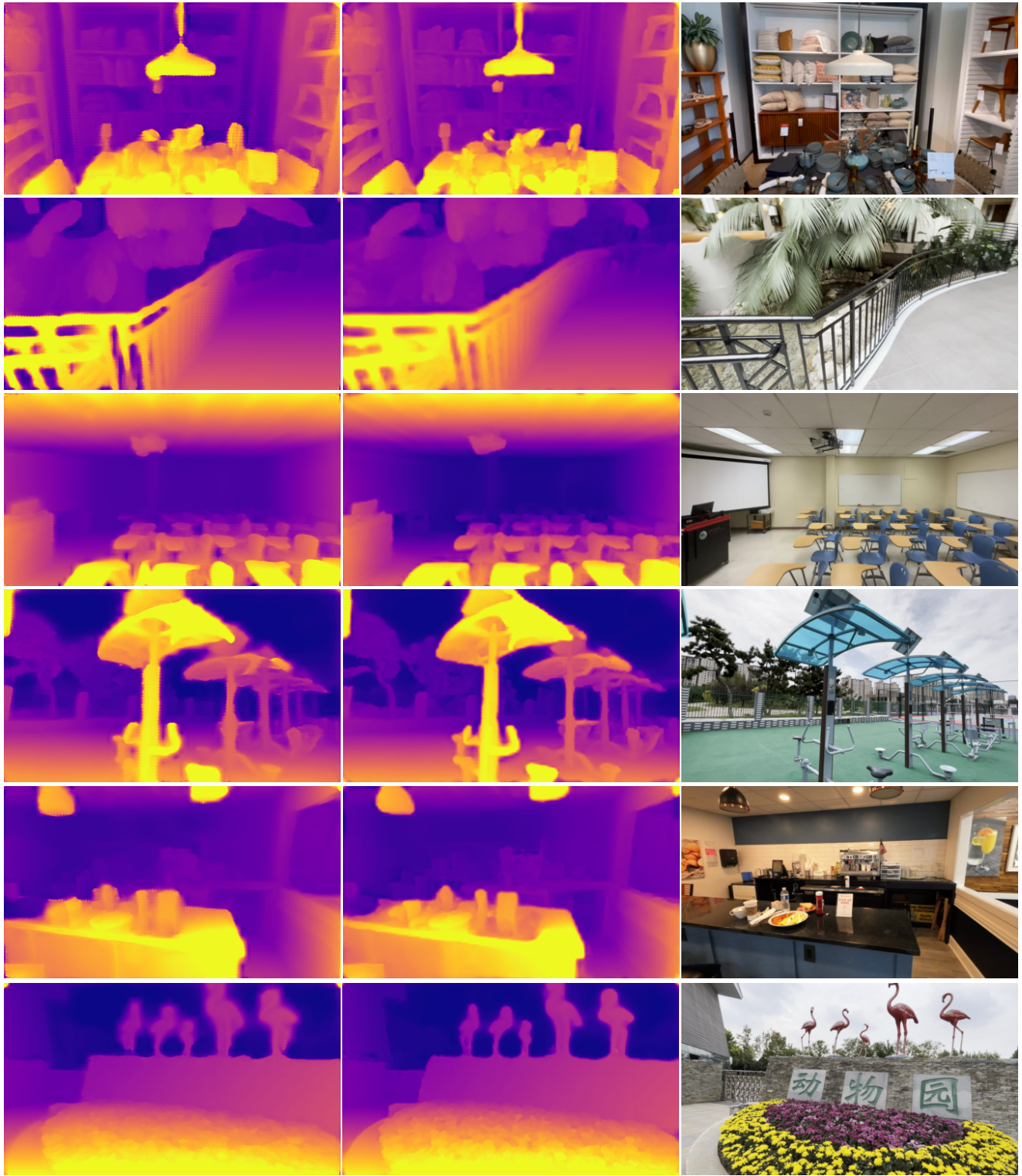


Figure 9. Comparison of depth prediction maps for different models on the RE10K dataset.



DepthSplat

IDESplat (Ours)

Reference

Figure 10. Comparison of depth prediction maps for different models on the DL3DV dataset.



Iteration 1

Iteration 2

Iteration 3

Reference

Figure 11. Visualization of intermediate depth prediction maps at different iterations in the IDESplat network.